# Photonic band gap of loop structure containing negative-index materials

Wei Tan,* Zhi Guo Wang, and Hong Chen
*Pohl Institute of Solid State Physics, Tongji University, Shanghai 200092, People's Republic of China*
(Received 3 November 2007; published 11 February 2008)

We predict the existence of a special photonic band gap in a quasi-one-dimensional loop structure containing negative-index materials in the subwavelength regime. The mechanism of the formation for this special band gap is quite different from the so-called zero-average-index gaps in the one-dimensional structures, due to the parallel action of the loop. The parallel action enhances the impedance contrast between the two parts on either side of the interface in each unit cell, thus resulting in strong reflection which increases the width of the band gap. In addition, we show that even large band gaps could be obtained in multichannel structures.

DOI: 10.1103/PhysRevE.77.026603 PACS number(s): 41.20.Jb, 42.70.Qs, 73.20.Mf, 78.20.Ci

Photonic band gap (PBG) materials [1] have received increased attention during the past two decades. Conventional PBGs originate from the interference of the Bragg scattering in a periodical dielectric structure [1]. The PBG frequency is inversely proportional to the lattice constant. Recently, there has been a great deal of interest in studying a novel class of media which has become known as negative-index materials (NIMs) [2–12]. The NIMs are characterized by simultaneous negative permittivity and permeability. Properties of NIMs were analyzed theoretically by Veselago nearly 40 years ago [2], but only recently were they demonstrated experimentally [6]. As was shown by Veselago, NIMs possess a number of unusual electromagnetic effects, such as negative refraction [4,9], reversed Doppler shift [10], and reversed Cerenkov radiation [11]. These anomalous features allow considerable control over light propagation and open the door for new approaches to a variety of applications [4,13].

The study of one-dimensional (1D) photonic crystals (PhCs) containing NIMs presents another type of PBG, zero-$\bar{n}$ gap [14–16], which is invariant upon length scale change. Recent studies also show that twisting a structure enables one to sculpt a microstructure which leads to the appearance of low frequency band gaps responsible for the effective negative refractive index [17]. In the search of large PBG materials, quasi-1D systems come into sight [18–21]. The comblike structure with branches constructed of NIM shows new allowed minibands or minigaps for the electromagnetic wave propagation [18], and the inverse structure whose backbone waveguide is of NIM and branches of positive index material provides a large gap invariant with scaling [19].

Another quasi-1D structure, which is different from the comb where the resonator is made of a loop instead of a side branch, exhibits results in comparison with the comblike structure. Thus so-called loop structure, whose band structure results from both the periodicity and the interference of the two arms of the loop, was studied in detail when its components are positive refractive index materials [20,21].

In this study, we discuss the loop structure containing NIMs. The transmission properties of such a structure have not been investigated before, to the best of our knowledge. A special band gap that is invariant with a change of scale length is obtained, the behavior of which is quite different from the so-called zero-average-index gaps of the one-dimensional structures and the comblike structures. It is shown that a new form of action, named *parallel action*, plays an important role in this structure. Moreover, our results can be well applied to multichannel systems.

The scheme of the loop structure is shown in Fig. 1. Each cell is composed of a slender segment of length $d_1$ connected to a loop of length $d_2+d_3$ (each loop is constructed of two arms of different lengths $d_2$ and $d_3$).

Our study is conducted with the help of the interface response theory [21,22]. In this theory, the Green's functions of a network structure can be obtained by the Green's functions of its elementary constituents. For the loop structure, by linear superposition of the corresponding elements associated to those of the slender segments and the loops, one deduces the $(3\times 3)$ matrix $[g(MM)]^{-1}$ associated with the unit cell with free ends,

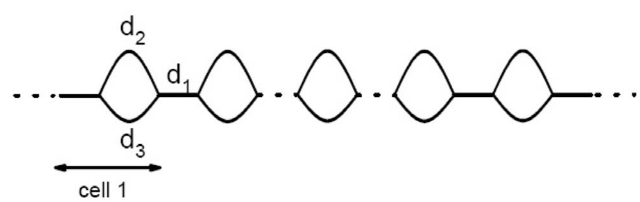


FIG. 1. Scheme of the loop structure.

*Corresponding author. zgwang@mail.tongji.edu.cn

 

$$[g(MM)]^{-1} = \begin{pmatrix} -\frac{F_1C_1}{S_1} & \frac{F_1}{S_1} & 0 \\ \frac{F_1}{S_1} & -\frac{F_1C_1}{S_1} - \frac{F_2C_2}{S_2} - \frac{F_3C_3}{S_3} & \frac{F_2}{S_2} + \frac{F_3}{S_3} \\ 0 & \frac{F_2}{S_2} + \frac{F_3}{S_3} & -\frac{F_2C_2}{S_2} - \frac{F_3C_3}{S_3} \end{pmatrix} \quad (1)$$

with $F_j = \sqrt{\varepsilon_j(\omega)}/\sqrt{\mu_j(\omega)}$ and $\alpha_j = (\omega/c)\sqrt{\varepsilon_j(\omega)}\sqrt{\mu_j(\omega)}$, where $S_j$ and $C_j$ $(j=1,2,3)$ are abbreviations of $\sin(\alpha_j d_j)$ and $\cos(\alpha_j d_j)$, respectively. The corresponding $(2\times 2)$ matrix $[g_j(MM)]^{-1}$ associated only to the two ends of this unit cell was finally found to be

$$[g_j(MM)]^{-1} = \begin{pmatrix} A_1 & A_2 \\ A_3 & A_4 \end{pmatrix}, \quad (2)$$

with

$$A_1 = F_1(F_1S_1S_2S_3 - F_2C_1C_2S_3 - F_3C_1C_3S_2), \quad (3)$$

$$A_2 = A_3 = F_1(F_2S_3 + F_3S_2), \quad (4)$$

$$A_4 = -F_1F_2C_1C_2S_3 - F_1F_3C_1C_3S_2 + F_2^2S_1S_2S_3 + F_3^2S_1S_2S_3 - 2F_2F_3S_1(C_2C_3 - 1). \quad (5)$$

For an infinite periodic structure, all the interface elements of the inverse Green's function $[g_\infty(MM)]^{-1}$ is an infinite tridiagonal matrix formed by linear superposition of the elements $[g_j(MM)]^{-1}$. Taking advantage of the translational periodicity of this system, the matrix $[g_\infty(MM)]^{-1}$ can be Fourier transformed. Then the dispersion relation can be obtained,

$$\cos(kd) = \frac{1}{F_2S_3 + F_3S_2}\left\{ -S_1S_2S_3\left(\frac{F_1^2 + F_2^2 + F_3^2}{2F_1}\right) + F_2C_1C_2S_3 + F_3C_1C_3S_2 + \frac{F_2F_3}{F_1}S_1(C_2C_3 - 1)\right\}, \quad (6)$$

where $kd$ is the Bloch wave phase. For a finite size structure, the transmittance $T$ is related to the elements of the Green's function $g$ of this system by the following expressions:

$$T_n = |2iF_0 g(1,n+1)|^2, \quad (7)$$

where $F_0$ is the relative admittance of the substrate and $n$ is the number of unit cells.

Suppose the slender segments (medium 1) in the loop structure are substituted by a NIM, whose electromagnetic parameters are assumed to be isotropic and dispersive,

$$\varepsilon_1(\omega) = \varepsilon_{10} - \frac{\alpha}{\omega^2}, \quad \mu_1(\omega) = \mu_{10} - \frac{\beta}{\omega^2}, \quad (8)$$

where $\omega$ is the frequency measured in GHz and $\varepsilon_{10}$, $\mu_{10}$, $\alpha$, and $\beta$ are positive constants. If $\varepsilon_1(\omega)$ and $\mu_1(\omega)$ are simultaneously negative, the corresponding refractive index $n_1(\omega) = -\sqrt{\varepsilon_1(\omega)\mu_1(\omega)}$ is negative too. In the following, we choose $\varepsilon_2=\varepsilon_3=4$ and $\mu_2=\mu_3=1$ for the positive index material, and $\varepsilon_{10}=1$, $\mu_{10}=1$, and $\alpha=\beta=100$ for the NIM. The frequency region where the refractive index is negative is from zero to 1.6 GHz.

We calculate the band structure and the transmission spectrum of the electromagnetic wave in this structure. In Fig. 2(a) we show the special band gap in the frequency region we are interested in, which remains invariant while changing the unit-cell size by a scaling factor. Figure 2(b) is the transmission spectrum of a finite size structure corresponding to the band structure in Fig. 2(a). In the frequency interval between the two gap edges, $\alpha_j d_j$ $(j=1,2,3)$ are small quantities, which suggests that this band gap is a subwavelength band gap. Moreover, in comparison with the zero-$\bar{n}$ gap in the 1D PhC with the same system parameters (in order to ensures that the two structures are of the same size, we consider the situation corresponding to a specific length of the loop $d_2=d_3$), this gap is obviously deeper and broader, as depicted in Fig. 3.

To illustrate the influence of the parallel channels on the transmission of the electromagnetic wave in this structure, we expand $\cos(\alpha_j d_j)$ and $\sin(\alpha_j d_j)$ in Taylor series,

$$\cos(\alpha_j d_j) = 1 - \frac{(\alpha_j d_j)^2}{2} + O[(\alpha_j d_j)^2],$$

$$\sin(\alpha_j d_j) = \alpha_j d_j + O(\alpha_j d_j), \quad (9)$$

and then obtain two equations which determine the positions of the gap edges,

$$\varepsilon_1(\omega)d_1 + (\varepsilon_2 d_2 + \varepsilon_3 d_3) = 0, \quad (10a)$$

$$\mu_1(\omega)d_1 + \frac{\mu_2 d_2 \mu_3 d_3}{\mu_2 d_2 + \mu_3 d_3} = 0. \quad (10b)$$

It can be seen that the low gap edge is determined by the dielectric parameters of the constituted materials, and the high gap edge by the magnetic parameters. In comparison with those of the 1D PhC [23],

$$\varepsilon_1(\omega)d_1 + \varepsilon_2 d_2 = 0, \quad (11a)$$

$$\mu_1(\omega)d_1 + \mu_2 d_2 = 0, \quad (11b)$$

and those of the comblike structure under the boundary condition $H=0$ [19],

$$\varepsilon_1(\omega)d_1 + \varepsilon_2 d_2 = 0, \quad (12a)$$

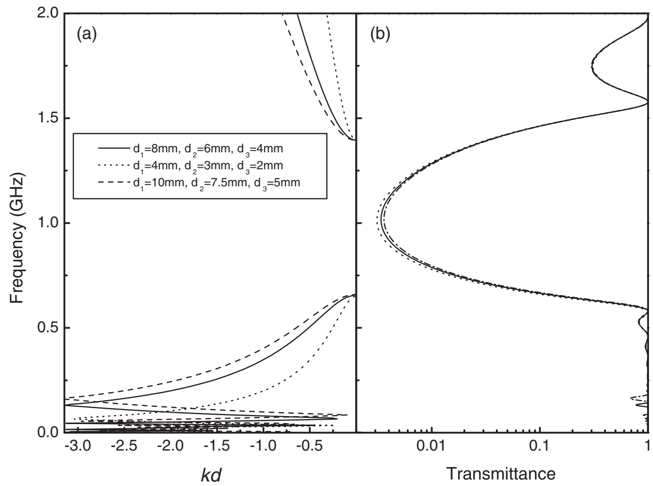


FIG. 2. (a) Invariance of the width of the special band gap with unit-cell size scaling. Solid line: $d_1$=8 mm, $d_2$=6 mm, and $d_3$=4 mm; dotted line: $d_1$, $d_2$, and $d_3$ are scaled by 1/2, respectively; dashed line: $d_1$, $d_2$, and $d_3$ are scaled by 5/4, respectively. (b) Transmittance through a finite size structure corresponding to the band structure in (a). These three structures are of the same total length. Solid line: 10 unit cells with $d_1$=8 mm, $d_2$=6 mm, and $d_3$=4 mm; dotted line: 20 unit cells with unit-cell size scaled by 1/2; dashed line: eight unit cells with unit-cell size scaled by 5/4.

$$\mu_1(\omega) = 0, \tag{12b}$$

the expressions of the loop structure are quite different. Equations. (11a) and (11b) indicate that the effective parameters of the 1D PhC can be given as spatial-averaged parameters, while Eqs. (12a) and (12b) show that the resonators of the comblike structure make a great contribution to the electric field in the backbone wave guide. For the loop structure,

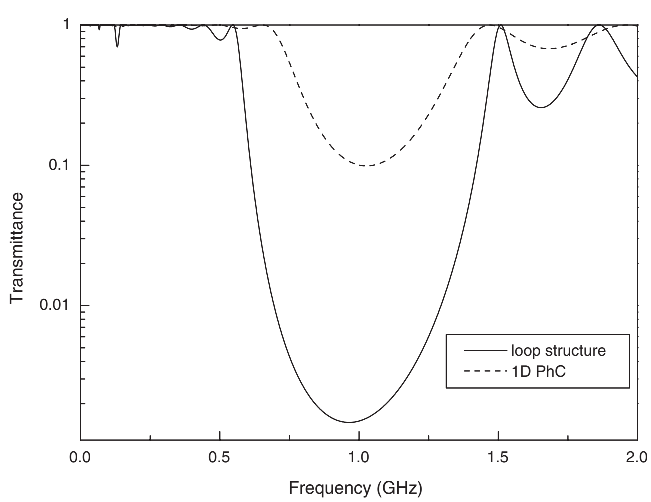


FIG. 3. Transmittance as a function of frequency through a finite size loop structure containing NIMs. Solid line: Loop structure; dashed line: 1D PhC; dotted line: comblike structure. They have identical parameters and the two arms of the loop are of the same length, $d_{\text{layer1}}=d_1$=8 mm and $d_{\text{layer2}}=d_2=d_3$=6 mm, and the number of the periodic cells is $n$=10.

the exhibition of the special relation between the two arms of the loop as

$$(\varepsilon d)_{\text{loop}} = \varepsilon_2 d_2 + \varepsilon_3 d_3, \tag{13a}$$

$$(\mu d)_{\text{loop}} = \frac{\mu_2 d_2 \mu_3 d_3}{\mu_2 d_2 + \mu_3 d_3}, \tag{13b}$$

suggests a new form of action—we call it parallel action. It can be understood that in the subwavelength regime, the two waves traveling along the two arms respectively are almost phase coincident, thus the interference between them could hardly open a band gap. We consider that this structure can be treated as homogeneous to good approximation. The two arms of the loop perform as parallel capacitors in response to the electric component of the electromagnetic wave, and parallel inductors to the magnetic component. This parallel action makes the effective impedance of the loop smaller than the intrinsic impedance of either of the two arms. The high impedance contrast results in strong reflection at the interface between the slender segment and the loop in each cell. This behavior ensures the capability of the loop structure to obtain a large band gap. As it is well known, the inhibition of electromagnetic modes, spontaneous emission, and zero-point fluctuations become more pronounced, when the PBG is made larger [21].

The width of this gap can also be enlarged easily through tuning system parameters. The frequencies corresponding to the low and high edges of this special gap are obtained by substituting in Eqs. (10a) and (10b) the expressions of $\varepsilon_1(\omega)$ and $\mu_1(\omega)$ from Eq. (8), respectively,

$$\omega_L = \sqrt{\frac{\alpha}{\varepsilon_{10} + \varepsilon_2 \frac{d_2}{d_1}\left(1 + \frac{\varepsilon_3}{\varepsilon_2}\frac{d_3}{d_2}\right)}}, \tag{14a}$$

$$\omega_H = \sqrt{\frac{\beta}{\mu_{10} + \mu_2 \frac{d_2}{d_1} \times \frac{1}{1 + \frac{\mu_2}{\mu_3}\frac{d_2}{d_3}}}}. \tag{14b}$$

When $\varepsilon_{10}$, $\varepsilon_2$, $\varepsilon_3$ increases or $\alpha$ decreases, the low gap-edge moves lower, and with smaller $\mu_{10}$ or bigger $\beta$, the high gap-edge moves higher. Once $d_2/d_1$ or $d_3/d_1$ increases, both edges move to lower positions, but the width of the band gap is still enlarged. Since the band gap is larger than that of the 1D PhC with the same system parameters, and the edges are more tunable than that of the comblike structure, the loop structure gains competitive advantages.

Furthermore, we move our attention to multichannel systems where each loop is substituted for more than two wires and $M$ describes the number of channels. The edges of the scaling invariant gap are

$$\varepsilon_1(\omega) d_1 + (\varepsilon d)_M = 0, \tag{15a}$$

$$\mu_1(\omega) d_1 + (\mu d)_M = 0, \tag{15b}$$

with

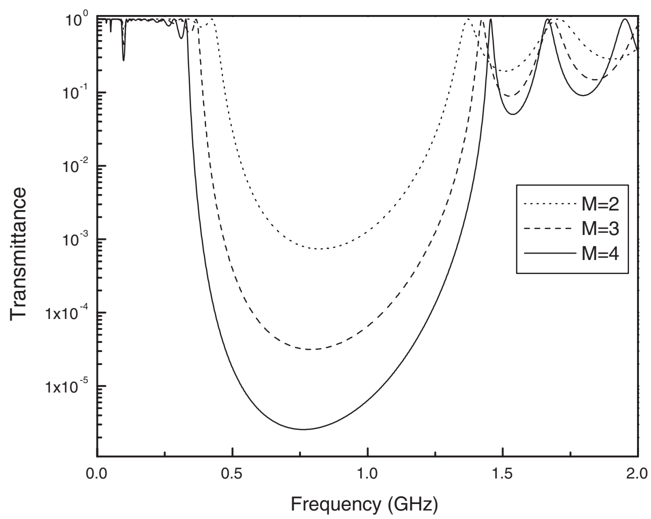


FIG. 4. Transmittance as a function of frequency through a finite size multichannel structure containing NIMs. Dotted line: $M=2$; dashed line: $M=3$; solid line: $M=4$. All the channels are of the same length, $d_1=8$ mm and $d_2=6$ mm, and the number of the periodic cells is $n=10$.

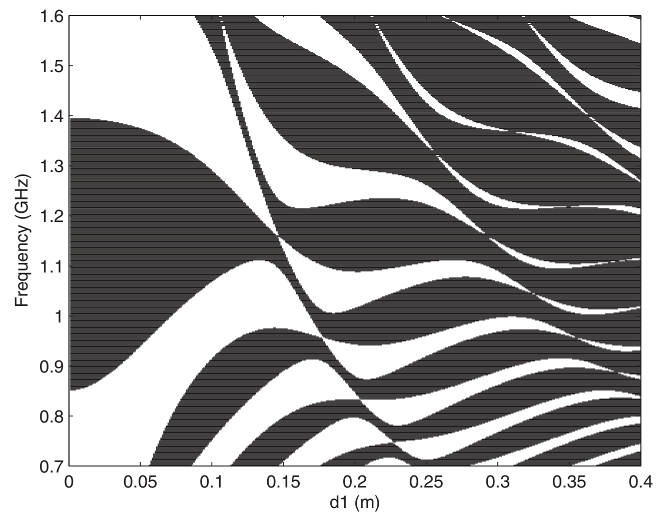


FIG. 5. Variance of the special band gap with unit-cell size enlarging. The shaded areas represent the band gaps of the loop structure. The ratio of $d_1$ to $d_2$ and that of $d_2$ to $d_3$ are kept as constant: $d_1/d_2=4/3$ and $d_2/d_3=3/2$.

$$(\varepsilon d)_M = \sum_{j=2}^{M+1} \varepsilon_j d_j$$

and

$$\frac{1}{(\mu d)_M} = \sum_{j=2}^{M+1} \frac{1}{\mu_j d_j} \quad (j=2,3,\ldots,M+1).$$

These results suggest that the parallel action is a universal action in the periodic structures containing more-than-one channels. In general, the loop structure is also a member of this group with $M=2$. In Fig. 4 we show how the band gap varies as $M$ increases. The calculations support our opinion that the band gap would be deeper and broader if there are more channels.

It is important to note that our calculation is conducted within the subwavelength limit. When this condition is not satisfied, Eqs. (10a), (10b), (11a), (11b), (12a), (12b), (13a), (13b), (14a), (14b), (15a), and (15b) will be invalid. Figure 5 shows that this special band gap becomes sensitive to scaling when the unit cell is large enough, and new gaps appear which are originated from the interference of the Bragg scattering at the interfaces and the interference of the parallel channels in each cell.

In conclusion, we have shown that the loop structure containing NIMs possesses a band gap which is invariant with length scaling. It has been shown that the behavior of its edges is quite different from those of the one-dimensional and the comblike structures due to the parallel action of the loop. From the analytical expressions of the gap edges, the width of this band gap can be easily enlarged through tuning system parameters. Moreover, we constructed multichannel structures based on the loop structure to obtain larger band gaps.

This work was supported by National Basic Research Program (973) of China under Grant No. 2006CB921701, National Natural Science Foundation of China under Grant No. 10634050, and Shanghai Science and Technology Committee.

[1] E. Yablonovitch, Phys. Rev. Lett. **58**, 2059 (1987); S. John, *ibid.* **58**, 2486 (1987).
[2] V. G. Veselago, Sov. Phys. Usp. **10**, 509 (1968).
[3] J. B. Pendry, A. J. Holden, D. J. Robbins, and W. J. Stewart, IEEE Trans. Microwave Theory Tech. **47**, 2075 (1999).
[4] J. B. Pendry, Phys. Rev. Lett. **85**, 3966 (2000).
[5] D. R. Smith, W. J. Padilla, D. C. Vier, S. C. Nemat-Nasser, and S. Schultz, Phys. Rev. Lett. **84**, 4184 (2000).
[6] R. A. Shelby, D. R. Smith, and S. Schultz, Science **292**, 77 (2001).
[7] D. R. Smith, J. B. Pendry, and M. C. K. Wiltshire, Science **305**, 788 (2004).
[8] P. Markos and C. M. Soukoulis, Phys. Rev. B **65**, 033401 (2001); Phys. Rev. E **65**, 036622 (2002).
[9] S. Foteinopoulou, E. N. Economou, and C. M. Soukoulis, Phys. Rev. Lett. **90**, 107402 (2003); A. A. Houck, J. B. Brock, and I. L. Chuang, *ibid.* **90**, 137401 (2003).
[10] E. J. Reed, M. Soljacic, and J. D. Joannopoulos, Phys. Rev. Lett. **91**, 133901 (2003).
[11] C. Luo, M. Ibanescu, S. G. Johnson, and J. D. Joannopoulos, Science **299**, 368 (2003).
[12] A. B. Movchan and S. Guenneau, Phys. Rev. B **70**, 125116

(2004).

[13] S. Guenneau, B. Gralak, and J. B. Pendry, Opt. Lett. **30**, 1204 (2005).

[14] J. Li, L. Zhou, C. T. Chan, and P. Sheng, Phys. Rev. Lett. **90**, 083901 (2003).

[15] H. T. Jiang, H. Chen, H. Q. Li, Y. W. Zhang, and S. Y. Zhu, Appl. Phys. Lett. **83**, 5386 (2003).

[16] S. B. Cavalcanti, M. de Dios-Leyva, E. Reyes-Gómez, and L. E. Oliveira, Phys. Rev. E **75**, 026607 (2007).

[17] A. Nicolet, A. B. Movchan, S. Guenneau, and F. Zolla, C. R. Mec. **334**, 91 (2006); A. Nicolet, A. B. Movchan, C. Geuzaine, F. Zolla, and S. Guenneau, Physica B **394**, 335 (2007).

[18] Gregorio H Cocoletzi, L. Dobrzynski, B. Djafari-Rouhani, H. AI-Wahsh, and D. Bria1, J. Phys.: Condens. Matter **18**, 3683 (2006).

[19] Y. Weng, Z. G. Wang, and H. Chen, Opt. Commun. **277**, 80 (2007).

[20] A. Mir, A. Akjouj, J. O. Vasseur, B. Djafari-Rouhani, N. Fettouhi, E. H. El Boudouti, L. Dobrzynski, and J. Zemmouri, J. Phys.: Condens. Matter **15**, 1593 (2003); E. H. El Boudouti, N. Fettouhi, A. Akjouj, B. Djafari-Rouhani, A. Mir, J. O. Vasseur, L. Dobrzynski, and J. Zemmouri, J. Appl. Phys. **95**, 1102 (2004).

[21] J. O. Vasseur, A. Akjouj, L. Dobrzynski, B. Djafari-Rouhani, and E. H. El Boudouti, Surf. Sci. Rep. **54**, 1 (2004).

[22] L. Dobrzynski, Surf. Sci. **180**, 489 (1987); **180**, 505 (1987).

[23] Y. Weng, Z. G. Wang, and H. Chen, Phys. Rev. E **75**, 046601 (2007).